



HAL
open science

Geometric Model Reduction Driven by Numerical Simulation Accuracy

Vincent Vadez, François Brunetti, Pierre Alliez

► **To cite this version:**

Vincent Vadez, François Brunetti, Pierre Alliez. Geometric Model Reduction Driven by Numerical Simulation Accuracy. ICES 2021 - International Conference on Environmental Systems, Jul 2021, Lisbon, Portugal. hal-03278653

HAL Id: hal-03278653

<https://inria.hal.science/hal-03278653>

Submitted on 5 Jul 2021

HAL is a multi-disciplinary open access archive for the deposit and dissemination of scientific research documents, whether they are published or not. The documents may come from teaching and research institutions in France or abroad, or from public or private research centers.

L'archive ouverte pluridisciplinaire **HAL**, est destinée au dépôt et à la diffusion de documents scientifiques de niveau recherche, publiés ou non, émanant des établissements d'enseignement et de recherche français ou étrangers, des laboratoires publics ou privés.

Geometric Model Reduction Driven by Numerical Simulation Accuracy

Vincent Vadez¹ and François Brunetti²
Dorea Technology, Sophia Antipolis, France

Pierre Alliez³
Université Côte d'Azur, Inria, France

ABSTRACT

When dealing with real-time simulation, radiative thermal computations have always been, and are still a challenge. Notably, computing view factors is very compute-intensive when the input 3D model is complex and exhibits many holes and occlusions. The task is even more difficult on complex geometries generated through topological optimization and on dense meshes required for finite element simulation. This paper focuses on geometric model reduction through mesh decimation. The decimation algorithm is made accurate to the radiative thermal simulation, in order to trade accuracy for computing times. More specifically, the input model is first decomposed into thermal nodes, then we estimate through radiative thermal simulation the sensitivity of decimating each thermal node against a maximum temperature tolerance. Such estimations are then utilized to render the entire mesh decimation process informed by the physical simulation. These estimations are relevant for predicting the amount of decimation applicable to each thermal node, given a user-defined maximum temperature tolerance.

I. INTRODUCTION

Accurate radiative thermal simulation is still a scientific challenge,¹ in particular due to the intrinsic complexity of computing view factors (quadratic in the number of facets of the geometric models). In addition, the geometric models of recent satellites are substantially more complex,² and real-time simulations are required for implementing digital twins.³ Numerical simulation of radiative phenomena via finite elements is often impossible on the original CAD models, and requires tessellations in the form of dense meshes. The resulting meshes (often conservative), are excessively complex from a geometric point of view and are in general not physics-informed.⁴ Model reduction is commonly performed to reduce either the number of thermal variables of the mathematical simulation model or the mesh complexity. Practitioners commonly perform time-consuming trial-and-error processes and the output reduced models are often far from the optimum.

On the one hand, mathematical model order reduction approaches offer the benefit to directly tackle the numerical equations, using assumptions and simplifications thanks to the physical expert knowledge of the system under study. Popular model order reduction methods include Proper Generalized Decomposition,⁵ Principal Component Analysis⁶ or Singular Value Decomposition.⁷ A major constraint in these approaches is that they rely heavily on mathematical and physical expertise to be reliable. On the other hand, geometric model reduction does not require any expertise in mathematics or physical simulation, but are disconnected from physics. The most common mesh reduction methods proceed by decimation through a series of edge collapse operators, whose order and degrees of freedom are governed by a geometric error metric.

A. State of the Art

Mathematical order reduction first appeared in the seventies, applied to fluid mechanics with the work of Lumley,⁸ involving large dynamical systems representing many physical phenomena at different scales (for Navier-Stokes equations, the number of degrees of freedom can go up to 10^6). New reduction methods were then devised for other simulations.

Modal synthesis methods⁹ consist in decomposing an object into a set of modes (eigen functions of the considered problem, depending on boundary conditions), which are then studied with Fourier analysis. Substructuring methods¹⁰ rely upon the analysis of the dynamic behavior of substructures separately, and then compute the assembled dynamics thanks to coupling procedures. Optimal methods decompose a physical field depending on

¹Ph.D. Student, Dorea Technology, 75 Chemin de l'Olivet, 06110 Le Cannet, FRANCE

²CEO, Dorea Technology, 75 Chemin de l'Olivet, 06110 Le Cannet, FRANCE

³Inria Senior Researcher, 2004 route des Lucioles BP 93 06902 Sophia-Antipolis, FRANCE

the factors that mostly impact the physical behaviors of the system, through e.g., computing a Singular Value Decomposition (SVD).

Geometric order reduction methods have been mainly developed in the geometric modeling community. The main objective of these methods is to preserve a specific error metric (such as volume, normal orientations or planarity) while reducing the number of mesh elements,¹¹⁻¹³ see Figure 1, 2 and 3. The main drawback of these methods is that they are physics unaware, so that the reduced geometric model can deteriorate important mathematical or physical properties. This motivates the need for a geometric model reduction method tailored to numerical simulations.

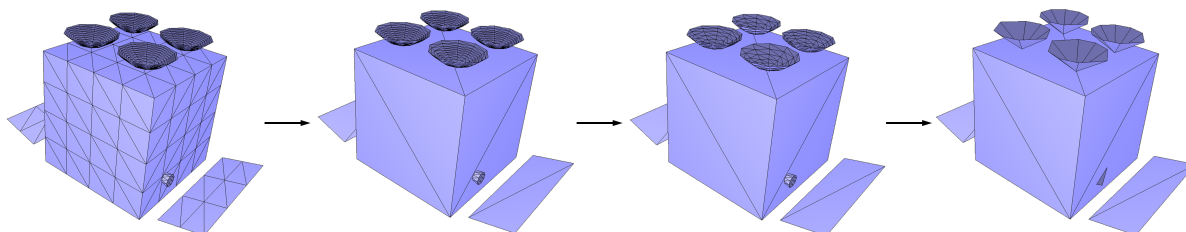


Fig. 1: Geometric reduction applied to a mesh. From left to right: input mesh, 25%, 50%, and 75% reduction.

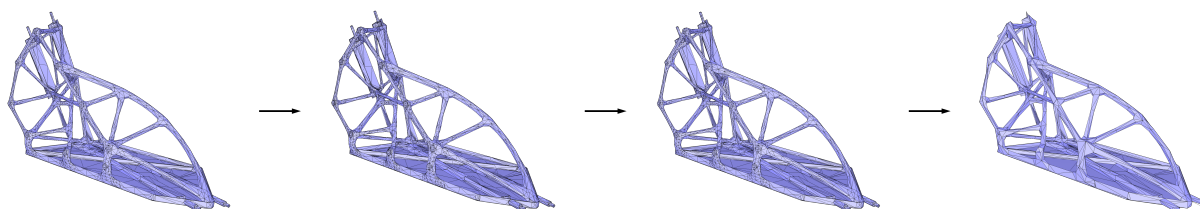


Fig. 2: Geometric reduction applied to a free-form mesh. From left to right: input mesh, 25%, 50% and 75% reduction.

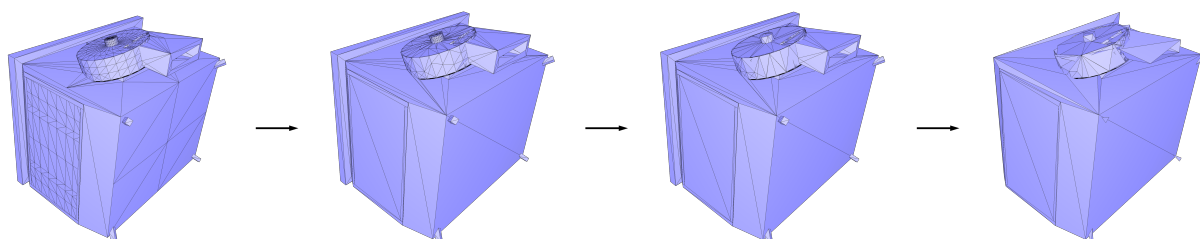


Fig. 3: Mesh decimation applied to a satellite part, where planarity is preserved. From left to right: input mesh, 25%, 50% and 75% reduction.

B. Positioning and contributions

This paper focuses on the problem of reducing the geometric model of a physical object which undergoes radiative thermal simulation, while preserving a desired physical property. This approach seeks to create a reduced model for real time simulation (at the end of the model construction process), dedicated to flight operation phases. The approach detailed here relies upon two main components: a geometric reduction process (oblivious to physics) and a simulation black box requested every n^{th} step of reduction, which yields changes in the physical property of interest (here a temperature difference). The considered simulation neglects specular behavior and is performed over a complete orbit for a given day of the year. A naive approach consists of performing the geometric reduction process until the maximum allowed temperature difference is reached or a given minimum number of meshes elements (vertices, edges, faces) is met. Our main contribution is to perform a sensitivity analysis for each thermal node, in order to perform a simulation-driven geometric reduction process. The method is first evaluated on a simple satellite mesh with no topological defects, and then on a real-world use case.

II. BACKGROUND

The focus is put on reduction for radiative thermal simulation of satellites. A satellite is exposed to extreme temperatures ranges and its equipments function only within specific temperature bounds. It is thus mandatory

to be as accurate as possible to the radiative surfaces during the reduction process, and eventually to the radiative thermal simulation.

Radiative heat transfer is a problem primarily governed by geometric view factors between surface mesh elements, with a quadratic complexity of computations in the number of faces of the mesh. Given two face elements 1 and 2, the (unobstructed) view factor from 1 to 2, a real number between zero and one referred to as $F_{1 \rightarrow 2}$, measures the proportion of the radiation which leaves 1 and strikes 2:

$$F_{1 \rightarrow 2} = \frac{1}{A_1} \int_{A_1} \int_{A_2} \frac{\cos \theta_1 \cos \theta_2}{\pi s^2} dA_2 dA_1, \quad (1)$$

where A_1 denotes the area of 1, s^2 denotes the squared distance from 1 to 2, and θ_1 denotes the angle between the normal vector of 1 and the segment between 1 and 2. For general surfaces, calculating accurate geometric view factors requires solving these integrals via quadrature methods. For complex scenes with many objects and obstacles such calculations are compute-intensive, preventing real-time simulations. Recently, a progressive method for computing view factors in order to best trade computation time for desired accuracy has been proposed.¹⁴ In this paper, the number of geometric elements (vertices, edges and faces) of the original mesh is reduced while preserving the numerical simulation as much as possible.

III. GEOMETRIC MODEL REDUCTION

A. Mesh Data Structure

Satellite or mechanical parts are commonly modeled via computer-aided design, yielding 3D models represented by NURBS surfaces. These models are then tessellated to enable physical simulation with finite elements. The tessellation process does not always generate as output oriented 2-manifold meshes (Fig.4), and these meshes are often non-conforming (edges and faces do not match exactly, see Figure 5, left). The input mesh is first rendered triangular and conforming via recursive edge bisection and conforming facet triangulation, see Figure 5, right. In order to deal with non-manifold meshes, a mesh data structure similar to the *AIF data structure*¹⁵ has been implemented.

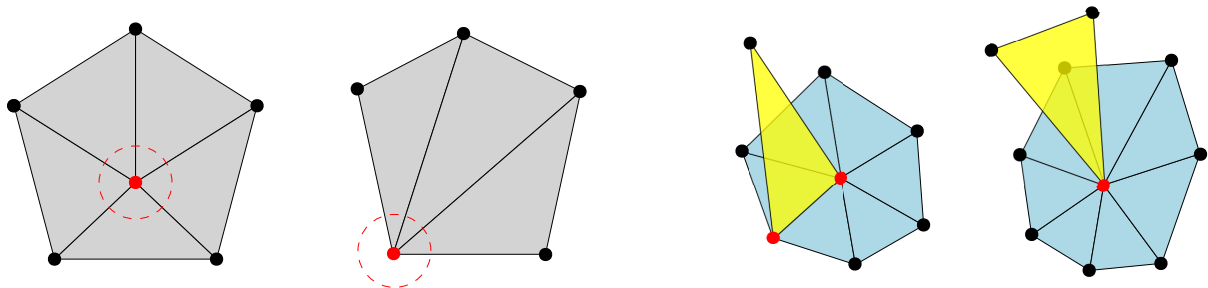


Fig. 4: Manifold and non-manifold meshes. The mathematical definition of 2-manifold is a topological space with the property that each point has a neighborhood that is homeomorphic to the Euclidean space of dimension 2. In a discrete setting, a mesh is considered manifold if each edge is incident to only one or two faces, and if the faces incident to a vertex form a single closed or open fan. Left: Manifold meshes. Right: Non-manifold meshes.

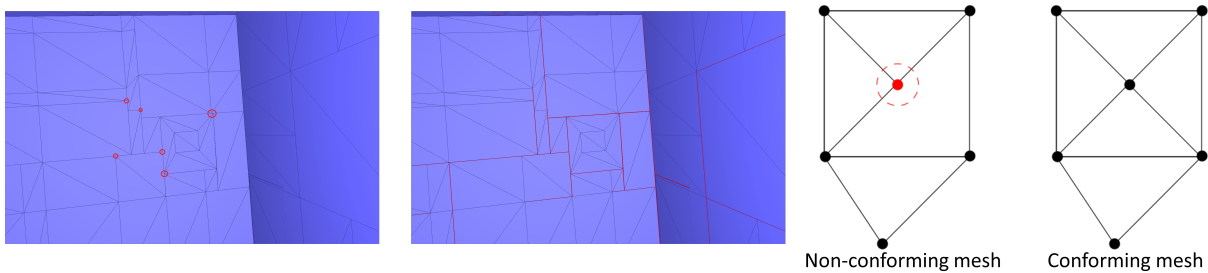


Fig. 5: Non-conforming mesh and conforming process. Left: non-conforming area (highlighted in red). Middle: Holes between faces of a mechanical part (highlighted in red). Right: Non-conforming then conforming mesh after recursive edge bisection and conforming facet triangulation.

B. Extracting the external geometry

As radiative heat transfer is proceeded on the external geometry of a satellite, extracting it from the input model is required. Most state-of-the-art methods rely upon ray shooting and intersections operations to obtain the visible geometry from a given point of view for a 2D or 3D model.^{16), 17} These algorithms are effective but become too compute-intensive for large and complex models, preventing real-time simulation. To address this problem, a GPU-based algorithm is proposed leveraging the Z-buffer. For multiple camera locations in the 3D space, renderings of the external faces oriented towards the camera are generated. When both camera and faces see each other (i.e., if the scalar product of their normals is positive), the faces are colored in different levels of gray depending on their distances from the camera Fig. 6. The colored faces from all camera viewpoints are collected to retrieve the full external geometry. Note that radiative heat transfer can also be directly computed with GPU implementations.¹⁸

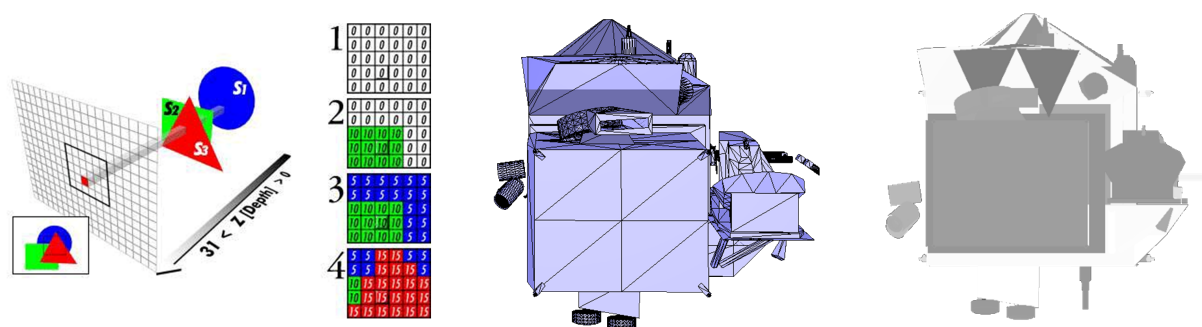


Fig. 6: Extracting the external geometry of a satellite. *Left: z-buffer principle. Middle: mesh view. Right: GPU-rendered view.*

The external geometry extraction process detailed above is applicable to other fields of study, such as reducing the computations time for solar powers received. It was observed that the number of faces has minor impact on the complexity of the calculation. The major computation factor lies into the definition of the projection which depends on the size of the object (for instance, a 10m x 2m satellite takes more time than a 3m x 2m satellite). This is explained by the number of pixels per area unit allocated for recognizing the external faces. A special care has been put to ensure that none of the faces are smaller than a minimum number of pixels. The algorithm can process objects with a very large number of faces.

The above process makes it possible to perform the calculation in 5 seconds per viewpoint, for a model with 100,000 triangles measuring 6m x 3m. The object undergoes a rotation on the 3 axes (in + and - direction on the 2 other axes) with a configurable cutting. The global calculation takes around 36 minutes, returning 40,000 external triangles in the end, see Fig. 7.

This algorithm has been adapted in order to calculate incident powers coming from a radiative source. Since the incident power of a face is the percentage of illumination that a face receives from an energy source (e.g., sun or albedo coming from the Earth), it depends on (1) the angle of the face with the source (a face perpendicular to the source receives nothing), (2) the occlusions with the other faces as well as (3) the direct reflection of the illumination of the faces on the others potentially not directly illuminated.

To perform the calculation of the illumination ratio, it is only required to know the number of pixels captured on the projected screen over the area of the face (units: $\frac{\text{pixel size} * \text{number of pixels}}{\text{area unit}}$). Computing the illumination of the faces by reflection requires knowing the view factors thus the ratio of illumination of the faces not directly illuminated.

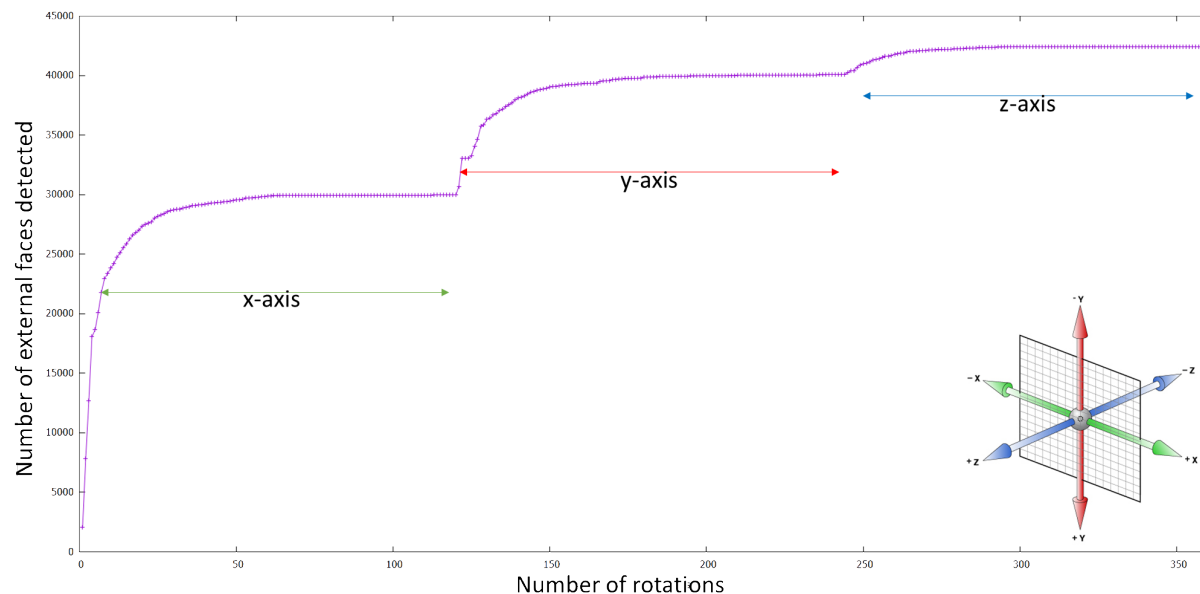


Fig. 7: Number of detected faces depending on the number of rotations applied. *The changes of axis are clearly visible.*

a) Preserve boundaries.: Specific physics may require to split the original model into sub-models to run the simulation, radiative simulation being no exception to this rule with the nodal breakdown. Applying a geometric model reduction to such cases imply reducing each sub-model apart from each others, and then reassemble them all into the global reduced one, while preserving physical boundaries. For instance, it is mandatory to not create holes in the satellite crate during the reduction process to avoid unwanted internal radiative exchanges coming from the outside. There is no need to rely upon radiative cavities in this case since the reduction is proceeded on the external geometry given by the above extraction algorithm, and the chosen decimation metric preserves the contours and areas of the sub-models, preventing holes from appearing.

IV. PHYSICS-UNAWARE REDUCTION

The proposed physics-unaware approach relies on a naive mesh reduction algorithm in which the clusters are uniformly reduced, i.e. with the same reduction ratio for each cluster. Fig. 8 depicts a satellite model (1K facets), before and after mesh reduction, the simulation performed being based on steady-state node-to-node radiative couplings. The material properties are considered uniform on all faces and no conductive simulation is proceeded, corresponding to a pure radiative scenario. However, and since we can preserve the topology and surfaces of the thermal nodes, conduction effects remain valid during the reduction. The mesh reduction process relies upon a volume-preserving error metric.¹² The latter is relevant since radiative thermal simulation is governed by view factors (purely geometric, depending on areas, orientations and distances), and the volume is also a product of area by distance. Such a naive approach yields clusters being too much approximated while others could still be reduced. This motivates the need for a physics-informed variant.

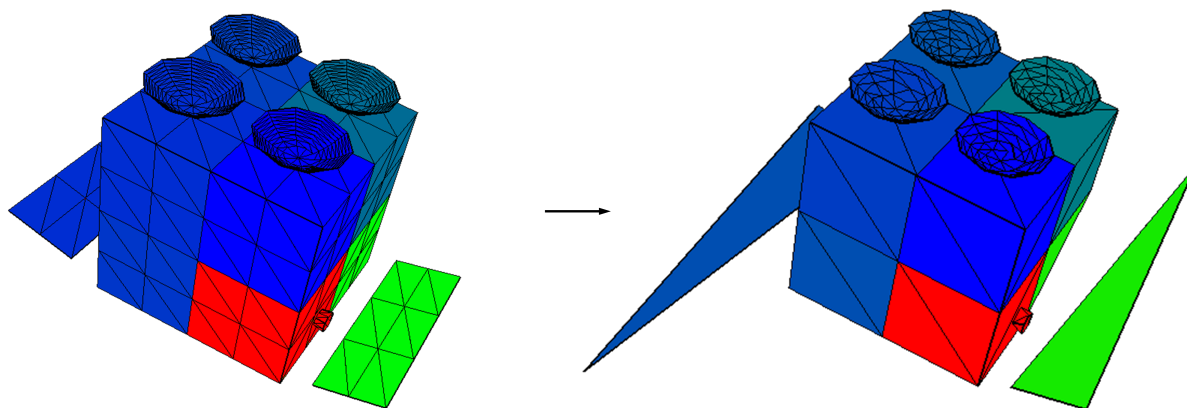


Fig. 8: Physics-unaware mesh reduction. *The maximum distortion tolerance (0.5 degrees) is reached when solar panels are heavily deteriorated, while the antennas can still be reduced (from 1006 to 370 facets).*

V. PHYSICS-INFORMED REDUCTION

In this paper the considered simulation is the radiative heat transfer applied to a satellite. The resolution of the equations being proceeded via nodal breakdown, see Fig. 9, the reduced model must preserve the same number of thermal nodes. The algorithm is decomposed into three main steps. The first step, referred to as clustering, splits the initial model into files containing clusters information (geometry and materials), creating one file per cluster. A cluster is then a set of faces with the same thermo-optical properties belonging to the same thermal node. Depending on the topology, in particular when opposite sides of the spacecraft can be considered independent, view surfaces can be used to improve the clustering provided that there is no shading. Clusters files are then sorted from smallest to largest in terms of number of faces. The second step, referred to as reduction, reduces every cluster in accordance to a global user-defined reduction ratio. If a cluster cannot be reduced as defined (for instance if the cluster is reduced to a single facet), the reduction deficit is applied to the next cluster, in order to meet the global defined decimation ratio. The third step consists in reassembling the reduced clusters into the full approximated model, and performing numerical simulation. These three steps are repeated until the maximal distortion tolerance is met, or if the geometric model can no longer be reduced.

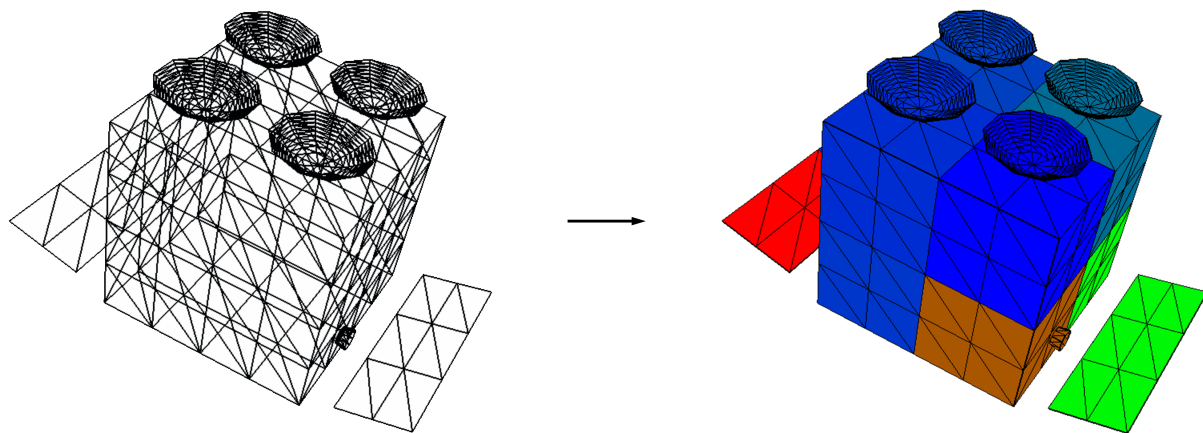


Fig. 9: Nodal breakdown (i.e., clustering) applied to radiative thermal simulation. *Left: geometric input model. Right: nodal breakdown and simulation output. The thermal nodes are depicted.*

A. Sensitivity Analysis

To instantiate the proposed physics-informed approach, a sensitivity analysis is first proceeded. In the heat transfer community, this method is commonly applied to compute radiative heat transfer on specific structures.^{19)–21)} In the considered context of this paper, a user-defined mesh reduction ratio is applied to each geometric cluster of the model (here a thermal node), perform the numerical simulation and check the temperature distortion for the whole model, the other clusters being unchanged. Such a reduction process is pursued for a series of increasing reduction ratios, until a maximum temperature difference is reached. Plotting temperature differences against reduction ratio offers a means to identify which parts of the satellite are sensitive to mesh reduction. See Fig. 10.

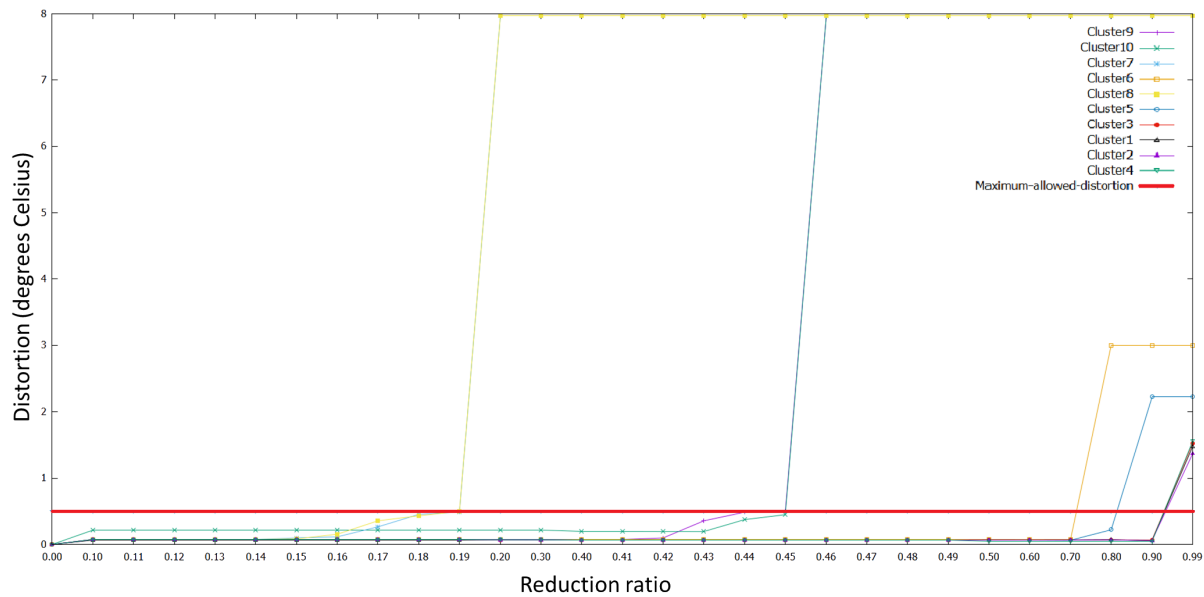


Fig. 10: Sensitivity analysis for each cluster of the considered model (clusters are sorted in the caption by size from smallest to largest). Some clusters quickly reach the maximum temperature difference while others can be further reduced without reaching it. The large difference jumps appear when a cluster’s shape is heavily deteriorated, not preserving anymore the original view surfaces of the cluster before decimation.

B. Prediction

For the sake of prediction, the above sensitive analysis curve is now utilized by choosing a maximum temperature difference target, and deducing the feasible mesh reduction ratio for each cluster. Fig. 11 plots the real difference against the target difference. It can be observed that the prediction is faithful, except for large differences where the distortion is underestimated. The latter is explained by the fact that the sensitivity analysis is performed on each cluster in isolation, while some clusters are coupled from the radiative simulation point of view.

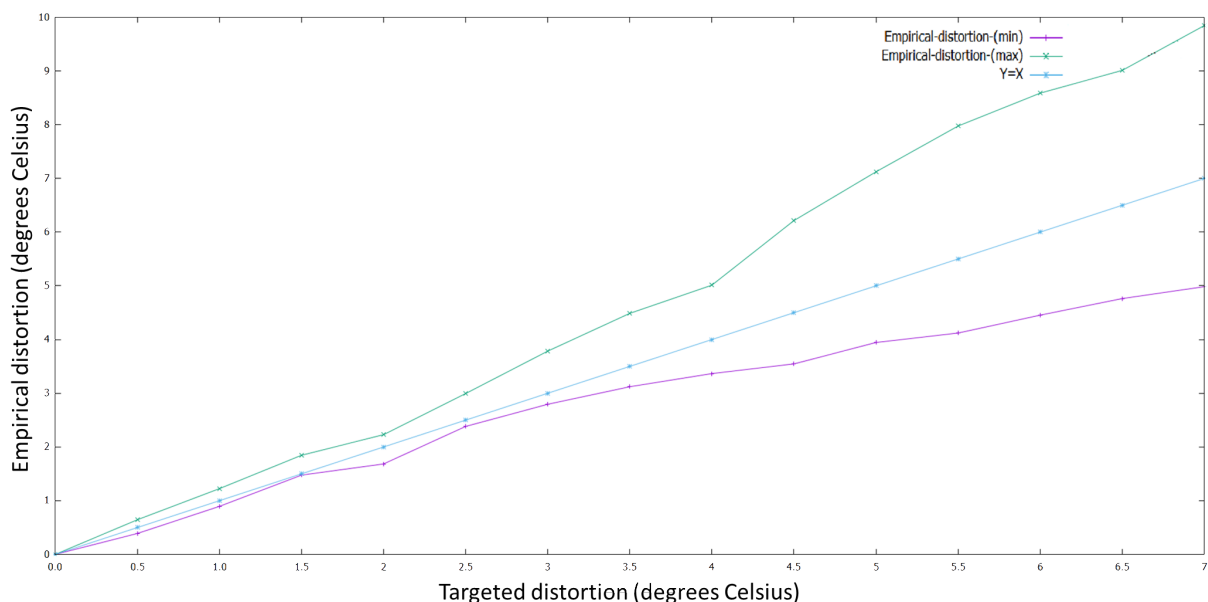


Fig. 11: Real difference against target difference (in degrees Celsius). Two plots are shown: the empirical difference right before exceeding the targeted difference (below the $Y=X$ straight line) and right after exceeding it (above the $Y=X$ straight line).

Fig. 12 depicts a thermal simulation applied to a model reduced with prediction. The maximum temperature difference compared to the original model is 0.0449 Celsius degrees.

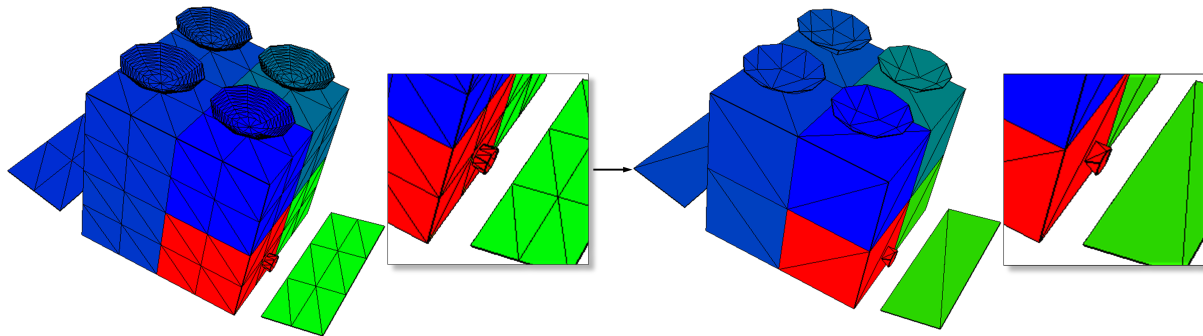


Fig. 12: Thermal simulation applied to a reduced model with prediction (from 1006 to 136 facets, i.e. a 90% reduction ratio).

Adding variable thermo-optical material properties is achieved by splitting a thermal node into sub-clusters each with a different material. It is observed that the predictions detailed above still hold in this case.

Figure 13 summarizes the overall reduction process.

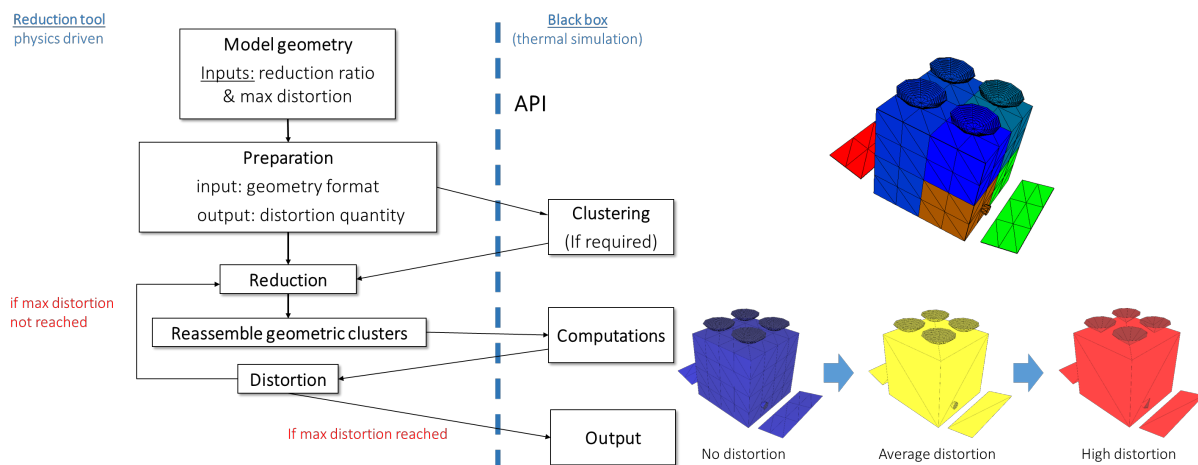


Fig. 13: Summary of reduction process. Left: mesh reduction. Right: numerical simulation.

VI. CONCLUSION

A mesh reduction process accurate to and driven by a numerical simulation has been proposed. The approach proceeds by performing a sensitivity analysis for each thermal node that translate into predictions of feasible reduction ratios given temperature difference tolerances. The thermal nodes are reduced in accordance to the said reduction ratios and reassembled to proceed with the global numerical simulation. The reduction process is pursued until the maximum allowed difference is reached (Fig. 13). A specific focus has been put on greatly reducing the number of geometrical elements while being faithful to the reference simulation values. A limitation of the proposed prediction approach is that finding the globally optimal reduced model for a given maximum temperature difference cannot be guaranteed. As a matter of fact, different approximated models can be obtained depending on the chosen geometric error metric, the initial conditions for the simulation and the geometric configuration of the satellite at a given time. As future work, another geometric error metric designed to best preserve the view factors between thermal nodes will be explored. Supervised learning will be explored used to find the error metric that best preserves the simulated differences. Recent advances based on fine-grained models (molecular dynamics, agent-based models)²² have been carried out for other simulated phenomena.

REFERENCES

- ¹ H. C. Hottel and A. F. Sarofim. *Radiation transfer (Mc Graw-Hill)*. Mc Graw-Hill, 1967.
- ² J. Becedas and A. Caparrós. Additive manufacturing applied to the design of small satellite structure for space debris reduction. In *Applications of Design for Manufacturing and Assembly*, 2018.

- ³ Thomas H.-J. Uhlemann, Christoph Schock, Christian Lehmann, Stefan Freiberger, and Rolf Steinhilper. The digital twin: Demonstrating the potential of real time data acquisition in production systems. *Procedia Manufacturing*, 9:113–120, 2017. 7th Conference on Learning Factories, CLF 2017.
- ⁴ Patrick Zulian. *Geometry-aware finite element framework for multi-physics simulations: an algorithmic and software-centric perspective*. PhD thesis, Università della Svizzera italiana, 2017.
- ⁵ F. Chinesta, A. Ammar, A. Leygue, and R. Keunings. An overview of the proper generalized decomposition with applications in computational rheology. *Journal of Non-Newtonian Fluid Mechanics*, 166(11):578–592, 2011. XVth International Workshop on Numerical Methods for Non-Newtonian Flows.
- ⁶ Ian T. Jolliffe and Jorge Cadima. Principal component analysis: a review and recent developments. *Philosophical Transactions of the Royal Society A: Mathematical, Physical and Engineering Sciences*, 374(2065):20150202, 2016.
- ⁷ Gene H Golub and Christian Reinsch. Singular value decomposition and least squares solutions. In *Linear algebra*, pages 134–151. Springer, 1971.
- ⁸ J. L. LUMLEY. The structure of inhomogeneous turbulent flows. *Atmospheric Turbulence and Radio Wave Propagation*, 1967.
- ⁹ B. Gaume, F. Joly, and O. Qummer. Modal reduction for a problem of heat transfer with radiation in an enclosure. *International Journal of Heat and Mass Transfer*, 141:779 – 788, 2019.
- ¹⁰ S. Abhinav, Debraj Ghosh, and C. S. Manohar. *Substructuring Methods for Finite Element Analysis*, pages 1–15. Springer Berlin Heidelberg, Berlin, Heidelberg, 2014.
- ¹¹ Michael Garland and Paul Heckbert. Surface simplification using quadric error metrics. *Proceedings of the ACM SIGGRAPH Conference on Computer Graphics*, 1997, 07 1997.
- ¹² Peter Lindstrom and Greg Turk. Fast and memory efficient polygonal simplification. In *Proceedings of the Conference on Visualization '98, VIS '98*, page 279286, Washington, DC, USA, 1998. IEEE Computer Society Press.
- ¹³ David Cohen-Steiner, Pierre Alliez, and Mathieu Desbrun. Variational Shape Approximation. Research Report RR-5371, INRIA, November 2004.
- ¹⁴ Vincent Vadez, François Brunetti, and Pierre Alliez. Progressive Geometric View Factors for Radiative Thermal Simulation. In *ICES 2020 - 50th International Conference on Environmental Systems*, Lisbon, Portugal, July 2020.
- ¹⁵ Frutuoso GM Silva and Abel JP Gomes. Aif - a data structure for polygonal meshes. In *International Conference on Computational Science and Its Applications*, pages 478–487. Springer, 2003.
- ¹⁶ Y. Zheng and K. Yamane. Ray-shooting algorithms for robotics. *IEEE Transactions on Automation Science and Engineering*, 10(4):862–874, 2013.
- ¹⁷ Danny Z. Chen and Haitao Wang. Visibility and ray shooting queries in polygonal domains. *Computational Geometry*, 48(2):31–41, 2015.
- ¹⁸ S. Silvestri and R. Pecnik. A fast gpu monte carlo radiative heat transfer implementation for coupling with direct numerical simulation. *Journal of Computational Physics: X*, 3:100032, 2019.
- ¹⁹ M. P. MENGIC and R. VISKANTA. A sensitivity analysis for radiative heat transfer in a pulverized coal-fired furnace. *Combustion Science and Technology*, 51(1-3):51–74, 1987.
- ²⁰ Eugene Ustinov. Sensitivity analysis of radiative heating and cooling rates in planetary atmospheres: General linearization and adjoint approaches. *European Geophysical Union*, 01 2002.
- ²¹ Joby Mackolil and Mahanthesh B. Sensitivity analysis of radiative heat transfer in casson and nano fluids under diffusion-thermo and heat absorption effects. *The European Physical Journal Plus*, 134, 12 2019.
- ²² Sebastian Kaltenbach and Phaedon-Stelios Koutsourelakis. Physics-aware, probabilistic model order reduction with guaranteed stability, 2021.